J|A|C|S
ARTICLES
Published on Web 10/17/2006

Picosecond Isomerization in Photochromic Ruthenium−Dimethyl Sulfoxide Complexes

Aaron A. Rachford and Jeffrey J. Rack*

Contribution from the Department of Chemistry and Biochemistry, Ohio University, Athens, Ohio 45701

Received June 12, 2006; E-mail: rackj@ohio.edu

Abstract: The complexes [Ru(tpy)(bpy)(dmso)]$(OSO_2CF_3)_2$ and *trans*-[Ru(tpy)(pic)(dmso)](PF_6) (tpy is 2,2′:6′,2″-terpyridine, bpy is 2,2′-bipyridine, pic is 2-pyridinecarboxylate, and dmso is dimethyl sulfoxide) were investigated by picosecond transient absorption spectroscopy in order to monitor excited-state intramolecular S→O isomerization of the bound dmso ligand. For $[Ru(tpy)(bpy)(dmso)]^{2+}$, global analysis of the spectra reveals changes that are fit by a biexponential decay with time constants of 2.4 ± 0.2 and 36 ± 0.2 ps. The first time constant is assigned to relaxation of the S-bonded ^{3}MLCT excited state. The second time constant represents both excited-state relaxation to ground state and excited-state isomerization to form *O*-$[Ru(tpy)(bpy)(dmso)]^{2+*}$. In conjunction with the S→O isomerization quantum yield ($\Phi_{S\rightarrow O} = 0.024$), isomerization of $[Ru(tpy)(bpy)(dmso)]^{2+}$ occurs with a time constant of 1.5 ns. For *trans*-$[Ru(tpy)(pic)(dmso)]^{+}$, global analysis of the transient spectra reveals time constants of 3.6 ± 0.2 and 118 ± 2 ps associated with these two processes. In conjunction with the S→O isomerization quantum yield ($\Phi_{S\rightarrow O} = 0.25$), isomerization of *trans*-$[Ru(tpy)(pic)(dmso)]^{+}$ occurs with a time constant of 480 ps. In both cases, the thermally relaxed excited states are assigned as terpyridine-localized ^{3}MLCT states. Electronic state diagrams are compiled employing these data as well as electrochemical, absorption, and emission data to describe the reactivity of these complexes. The data illustrate that rapid bond-breaking and bond-making reactions can occur from ^{3}MLCT excited states formed from visible light irradiation.

Introduction

A primary concern in the study and formation of photochemical excited states is the ability to access the stored energy in these states. By the nature of the short lifetimes typically associated with many of these states, reactions involving this stored potential energy must necessarily be rapid. One attraction of $[Ru(bpy)_3]^{2+}$-type (bpy is 2,2′-bipyridine) chromophores is the relatively long-lived excited state in aqueous and organic solvents ($\tau \approx 0.6-1.0$ μs).[1] Indeed, much effort has been dedicated toward extending these lifetimes in hopes of more efficiently accessing the energy stored in these excited states. More recently, a number of groups have investigated the formation of the charge-separated ^{3}MLCT (metal-to-ligand charge-transfer) state in $[Ru(bpy)_3]^{2+}$ and related complexes in hopes of better understanding the relationship between electronic localization and nuclear motion.[2−10] Improved understanding of these events will provide strategies for the development of improved photosensitizers for light-driven reactions.

Photoinduced or phototriggered molecular isomerizations employ the stored energy in an electronic excited state for rapid bond-breaking and bond-making reactions. One of the most well-studied examples of this type of reaction is photoisomerization of stilbene and its derivatives, where phenyl group rotation occurs following $\pi^*\leftarrow\pi$ excitation on an ultrafast time scale.[11−15] Photoinduced molecular motions such as those observed in stilbene are uncommon in inorganic or coordination chemistry, though the recent advances in molecular machines involving the sophisticated movements of rotaxanes and catenanes demonstrate the promise of this field.[16−19] Another area showing promise, which involves phototriggered molecular motions, is that of excited-state linkage isomerization of metal-bound ligands.[20−22]

(1) Juris, A.; Balzani, V.; Barigelletti, F.; Campagna, S.; Belser, P.; Von Zelewsky, A. *Coord. Chem. Rev.* **1988**, *84*, 88−277.
(2) Damrauer, N. H.; Cerullo, G.; Yeh, A.; Boussie, T. R.; Shank, C. V.; McCusker, J. K. *Science* **1997**, *275*, 54−87.
(3) Damrauer, N. H.; McCusker, J. K. *J. Phys. Chem. A* **1999**, *103*, 8440−8446.
(4) Yeh, A. T.; Shank, C. V.; McCusker, J. K. *Science* **2000**, *289*, 935−938.
(5) Bhasikuttan, A. C.; Suzuki, M.; Nakashima, S.; Okada, T. *J. Am. Chem. Soc.* **2002**, *124*, 8398−8405.
(6) McFarland, S. A.; Lee, F. S.; Cheng, K. A. W. Y.; Cozens, F. L.; Schepp, N. P. *J. Am. Chem. Soc.* **2005**, *127*, 7065−7070.
(7) Wallin, S.; Davidsson, J.; Modin, J.; Hammarstrom, L. *J. Phys. Chem. A* **2005**, *109*, 4697−4704.
(8) Gawelda, W.; Johnson, M.; de Groot, F. M. F.; Abela, R.; Bressler, C.; Chergui, M. *J. Am. Chem. Soc.* **2006**, *128*, 5001−5009.
(9) Monat, J. E.; McCusker, J. K. *J. Am. Chem. Soc.* **2000**, *122*, 4092−4097.
(10) McCusker, J. K. *Acc. Chem. Res.* **2003**, *36*, 876−887.
(11) Allen, M. T.; Whitten, D. G. *Chem. Rev.* **1989**, *89*, 1691−1702.
(12) Waldeck, D. H. *Chem. Rev.* **1991**, *91*, 415−436.
(13) Tamai, N.; Miyasaka, H. *Chem. Rev.* **2000**, *100*, 1874−1891.
(14) Natansohn, A.; Rochon, P. *Chem. Rev.* **2002**, *102*, 4139−4175.
(15) Liu, R. S. H.; Hammond, G. S. *Photochem. Photobiol. Sci.* **2003**, *2*, 825−844.
(16) Hubin, T. J.; Busch, D. H. *Coord. Chem. Rev.* **2000**, *200−202*, 5−52.
(17) Balzani, V.; Credi, A.; Ferrer, B.; Silvi, S.; Venturi, M. *Top. Curr. Chem.* **2005**, *262*, 1−27.
(18) Moonen, N. N. P.; Flood, A. H.; Fernandez, J. M.; Stoddart, J. F. *Top. Curr. Chem.* **2005**, *262*, 99−132.
(19) Collin, J.-P.; Heitz, V.; Sauvage, J.-P. *Top. Curr. Chem.* **2005**, *262*, 29−62.

10.1021/ja0641305 CCC: $33.50

Chart 1. Structures of Photoisomerizable Ruthenium−dmso Compounds

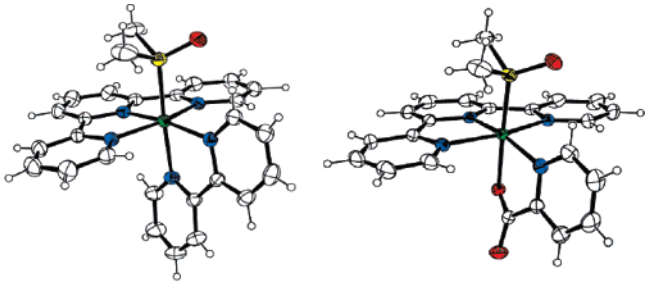

[Ru(tpy)(bpy)(dmso)]$^{2+}$ *trans*-[Ru(tpy)(pic)(dmso)]$^{+}$

Our efforts in the field of phototriggered molecular rearrangements have focused on excited-state S→O isomerizations of dimethyl sulfoxide (dmso).[23−28] Recently, we reported exceptionally large quantum yields of isomerization ($0.024 < \Phi_{S\rightarrow O} < 0.80$) for a series of ruthenium−polypyridine−dmso complexes of the general formula $[Ru(tpy)(L2)(dmso)]^{n+}$, where tpy is 2,2′:6′,2″-terpyridine and L2 is a variable bidentate ligand.[25,26,28] Large quantum yields of isomerization are indicative of electronic structures that efficiently access the stored energy within an excited state. These reactions represent fundamental examples of converting photonic energy into potential energy, which is subsequently employed for bond formation. For $[Ru(tpy)(bpy)(dmso)]^{2+}$ and *trans*-$[Ru(tpy)(pic)(dmso)]^{+}$ (pic is 2-pyridinecarboxylate, Chart 1), excited-state S→O isomerization is thought to be quite rapid, due to the subnanosecond lifetimes associated with the S-bonded excited states.[26,28] Herein we report our results from picosecond transient absorption spectroscopy and show direct observation of excited-state S→O isomerization of a bound dmso ligand.

Experimental Section

The complexes $[Ru(tpy)(bpy)(dmso)](OSO_2CF_3)_2$, $[Ru(tpy)(bpy)(dms)](OSO_2CF_3)_2$, *trans*-$[Ru(tpy)(pic)(dmso)](PF_6)$, and *trans*-$[Ru(tpy)(pic)(dms)](PF_6)$, where dms is dimethyl sulfide, were prepared as described elsewhere.[25,26] The trans isomer refers to the geometry of the picolinate carboxylate group and dmso. Both of the picolinate complexes containing dmso and dms exhibit this geometry. Electrochemical data and time-resolved and steady-state absorption measurements were collected in propylene carbonate. Spectroelectrochemical experiments were performed in argon-sparged propylene carbonate with 0.1 M *n*-tetrabutylammonium hexafluorophosphate ($TBAPF_6$) as the electrolyte. Chronocoulometric experiments were performed with a CH Instruments 730A electrochemical workstation while obtaining UV−visible spectra (Agilent HP 8452A UV−visible spectrometer) intermittently until 5% of charge remained. The target voltage was −1.3 and −1.4 V for reduced terpyridine in the bpy and pic complexes, respectively. The background spectra in both cases were the ground-state Ru(II) spectra. Picosecond transient absorption spectra were acquired at the Ohio Laboratory for Kinetic Spectrometry (OLKS) as part of Bowling Green State University's (BGSU) Center for Photochemical Studies. The experimental details were described previously, and only a brief discussion is provided here.[29−31] A Spectra-Physics Hurricane Evolution and Ti:sapphire were combined to yield 800 nm pulses of 130 fs in duration at a rate of 1 kHz. The excitation wavelength of 400 nm (∼2 μJ/pulse) was obtained from frequency-doubling the Ti:sapphire fundamental. A portion of the 800 nm fundamental was employed to generate the white light continuum probe source by focusing the light through either an ethylene glycol flow-through cell or a 3 mm thick sapphire plate. Detection from ∼450 to 750 nm was achieved with a double CCD spectrograph. Transient spectra at a particular delay time represent the average of 4000 excitation pulses. The instrument is operated through an in-house (BGSU) LabVIEW software routine. Kinetic analysis of the data was performed at Ohio University (OU) with the SPECFIT (version 3.0.37, Spectrum Software Associates) program, a global analysis routine based on single value decomposition. Goodness-of-fit was evaluated qualitatively by inspection of the residual plots. Nanosecond transient absorption spectra were collected at OU on a modified Edinburgh Instruments PS700 nanosecond transient absorption spectrometer, with 1.25 GHz, 500 Ms/s Tektronix DSO. The pump beam was provided by a SpectraPhysics Nd:YAG pumped OPO laser (1−3 mJ/pulse), while the probe beam was a Xe arc lamp. The pump−probe geometry was 90°. Analysis of single-wavelength kinetic traces was performed with a software program provided by Edinburgh Instruments.

Table 1. Absorption Maxima, Reduction Potentials,[a] and Isomerization Quantum Yields

	$[Ru(tpy)(bpy)(dmso)]^{2+}$	$[Ru(tpy)(pic)(dmso)]^{+}$
λ_{max} (S)	412 nm	419 nm
λ_{max} (O)	476 nm	518 nm
$E^{\circ\prime}_S$ ($Ru^{3+/2+}$)	1.49 V	1.31 V
$E^{\circ\prime}_O$ ($Ru^{3+/2+}$)	0.89 V	0.57 V
$E^{\circ\prime}_1$ ($L^{0/-}$)[b]	−1.20 V	−1.30 V
$E^{\circ\prime}_2$ ($L^{0/-}$)[c]	−1.58 V	−1.86 V
$\Phi_{S\rightarrow O}$	0.024 ± 0.001	0.25 ± 0.01

[a] Potentials referenced to Ag/AgCl in propylene carbonate with 0.1 M $TBAPF_6$. [b] This couple represents the terpyridine$^{0/-}$ couple. [c] This couple represents the picolinate$^{-/2-}$ couple.

Results

Shown in Table 1 are absorption maxima, reduction potentials, and quantum yields of S→O isomerization for $[Ru(tpy)(bpy)(dmso)]^{2+}$ and *trans*-$[Ru(tpy)(pic)(dmso)]^{+}$.[26] The geometry label refers to the relationship between the carboxylate group and dimethyl sulfoxide. The absorption maxima for the S-bonded isomers are 412 and 419 nm, while the absorption maxima for the O-bonded isomers are 476 and 518 nm, for the bpy and pic complexes, respectively (Figure 1). Voltammetric data reveal S-bonded $Ru^{3+/2+}$ reduction potentials at 1.49 and 1.31 V and O-bonded $Ru^{3+/2+}$ reduction potentials at 0.89 and 0.57 V vs Ag/AgCl for the bpy and pic complexes, respectively. Two distinct one-electron ligand reduction potentials are observed at −1.20 and −1.58 V for the bpy complex and at −1.30 and −1.86 V vs Ag/AgCl for the pic complex. The first ligand reduction is assigned to the terpyridine ligand in both

(20) Coppens, P.; Novozhilova, I.; Kovalevsky, A. *Chem. Rev.* **2002**, *102*, 861−883.
(21) To, T. T.; Barnes, C. E.; Burkey, T. J. *Organometallics* **2004**, *23*, 2708−2714.
(22) Yeston, J. S.; To, T. T.; Burkey, T. J.; Heilweil, E. J. *J. Phys. Chem. B* **2004**, *108*, 4582−4585.
(23) Rack, J. J.; Winkler, J. R.; Gray, H. B. *J. Am. Chem. Soc.* **2001**, *123*, 2432−2433.
(24) Rack, J. J.; Mockus, N. V. *Inorg. Chem.* **2003**, *42*, 5792−5794.
(25) Rack, J. J.; Rachford, A. A.; Shelker, A. M. *Inorg. Chem.* **2003**, *42*, 7357−7359.
(26) Rachford, A. A.; Petersen, J. L.; Rack, J. J. *Inorg. Chem.* **2005**, *44*, 8065−8075.
(27) Mockus, N. V.; Petersen, J. L.; Rack, J. J. *Inorg. Chem.* **2006**, *45*, 8−10.
(28) Rachford, A. A.; Petersen, J. L.; Rack, J. J. *Inorg. Chem.* **2006**, *45*, 5953−5960.
(29) Nikolaitchik, A. V.; Korth, O.; Rodgers, M. A. J. *J. Phys. Chem. A* **1999**, *103*, 7587−7596.
(30) Pelliccioli, A. P.; Henbest, K.; Kwag, G.; Carvagno, T. R.; Kenney, M. E.; Rodgers, M. A. J. *J. Phys. Chem. A* **2001**, *105*, 1757−1766.
(31) Okhrimenko, A. N.; Gusev, A. V.; Rodgers, M. A. J. *J. Phys. Chem. A* **2005**, *109*, 7653−7656.

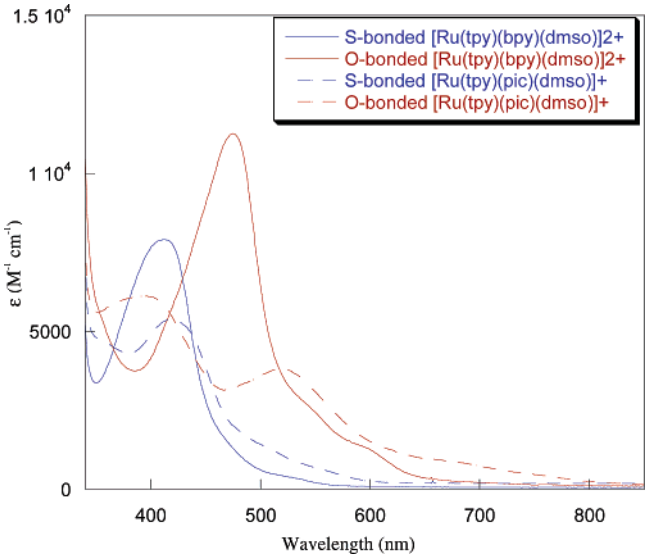

Figure 1. Absorption spectra of S- and O-bonded isomers of [Ru(tpy)(bpy)(dmso)]$^{2+}$ and [Ru(tpy)(pic)(dmso)]$^{+}$ in propylene carbonate.

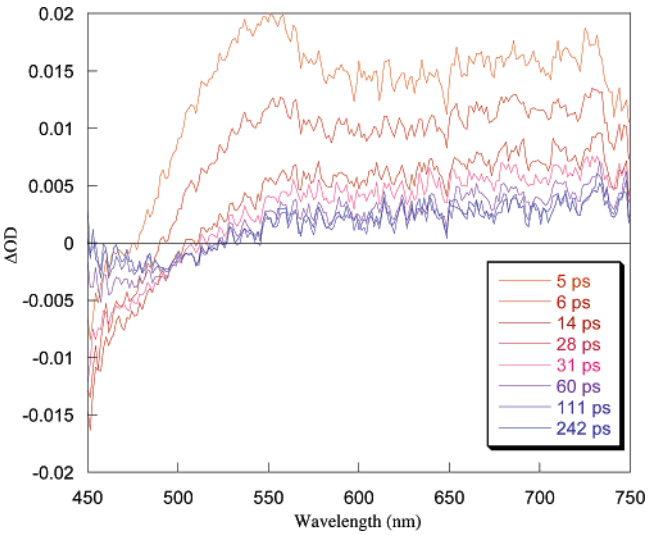

Figure 2. Selected transient absorption spectra of S-bonded [Ru(tpy)(bpy)(dmso)]$^{2+}$ in propylene carbonate solution.

complexes, whereas the second ligand reduction is assigned to the bipyridine and picolinate ligands, respectively. These values are in accord with literature values.[1] The difference in energy between metal-based oxidations and the first ligand reduction roughly matches the absorption energy for the S-bonded (*S*) and O-bonded isomers (*O*). The isomerization quantum yield ($\Phi_{S\rightarrow O}$) for the bpy and pic complexes is 0.024 and 0.25, respectively.

Shown in Figure 2 are selected traces at time delays ranging from 5 to 242 ps for *S*-[Ru(tpy)(bpy)(dmso)]$^{2+}$ ($\Phi_{S\rightarrow O} = 0.024$). For the S-bonded data, the first trace, at 5 ps, shows a weak bleach or negative peak near 450 nm, which corresponds to the red-edge of the ground-state absorption of the S-bonded isomer. This trace also features a sharp absorption near 550 nm and a broad, less-intense absorption at longer wavelengths ($\lambda > \sim 600$ nm). From 5 to 14 ps, the bleach near 450 nm becomes more pronounced, and the sharp absorption at 550 nm shifts to lower energy and becomes indistinguishable from the broad, featureless low-energy absorption ($\lambda > \sim 600$ nm). From 14 to 242 ps, the spectra show a loss of the bleach feature near 450 nm

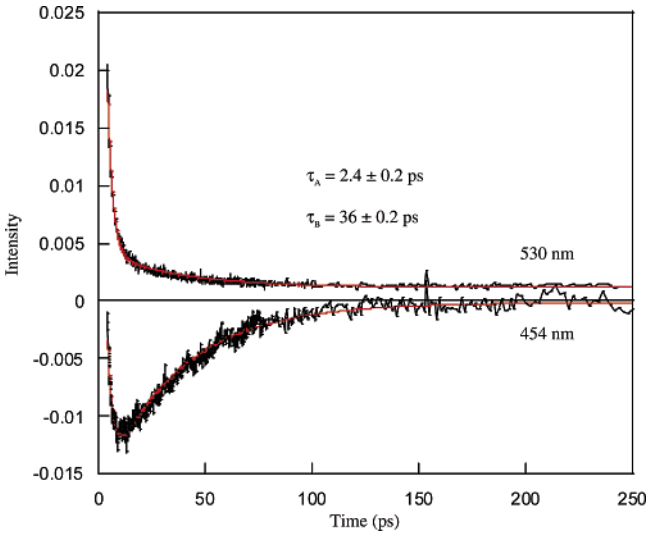

Figure 3. Single-wavelength kinetic traces (black) and biexponential fit (red) from global fitting analysis of [Ru(tpy)(bpy)(dmso)]$^{2+}$.

as well as subtle changes in the intensity of the low-energy absorption. The final spectrum of weak intensity shows a shallow bleach centered near 475 nm and a broad absorption at low energy ($\lambda > 550$ nm). Interestingly, an isosbestic point at 500 nm becomes apparent in the spectra from 14 to 242 ps. Monitoring the spectral changes at 454 and 530 nm reveals a biexponential decay with time constants of 2.4 ± 0.2 and 36 ± 0.2 ps (Figure 3).

The data for the O-bonded isomer (Supporting Information) were collected from a solution of the S-bonded isomer that had been photolyzed to prepare *O*-[Ru(tpy)(bpy)(dmso)]$^{2+}$. The O-bonded data reveal the evolution of an equilibrated excited state that is monoexponential with a time constant of 10.4 ± 0.2 ps, as determined by analysis of the spectral changes at 468 and 650 nm. The minimum in the transient spectrum near 475 nm corresponds well with the absorption maximum of *O*-[Ru(tpy)(bpy)(dmso)]$^{2+}$ as well as the final trace observed in the *S*-[Ru(tpy)(bpy)(dmso)]$^{2+}$ picosecond spectra. Further changes in the picosecond transient absorption spectra of either isomer are not observed after ~250 ps. The lifetime of excited-state *O*-[Ru(tpy)(bpy)(dmso)]$^{2+}$ is 8.3 ± 0.1 ns, as measured by nanosecond transient absorption spectroscopy (Supporting Information).

Spectral changes of *S*-[Ru(tpy)(pic)(dmso)]$^{+}$ ($\Phi_{S\rightarrow O} = 0.25$) are shown in Figure 4. The first trace, at 5 ps, features a sharp excited-state absorption at 470 nm and two broader absorptions at 575 and 700 nm. From 5 to 20 ps, the absorption at 470 nm decreases in intensity, while the two lower-energy absorptions show little change during this time. In addition, a weak negative peak is observed near 460 nm, corresponding to the red-edge of the ground-state absorption. Spectral changes from 20 to 807 ps reveal an isosbestic point ($\lambda \approx 475$ nm) and the formation of a broad absorption centered near 630 nm. The two broad, low-energy absorptions at 575 and 700 nm yield to the 630 nm absorption over this time. Kinetic analysis of the spectral changes at 462 and 660 nm reveals a triexponential decay with time constants of 3.6 ± 0.2 and 118 ± 2 ps, as well as a third, slower component of ~5.9 ns (Figure 5). The error on this last time component is large, but its presence is required for fitting. Analysis of *O*-[Ru(tpy)(pic)(dmso)]$^{+}$ shows the formation of an equilibrated excited state with a time constant of 8 ± 0.2

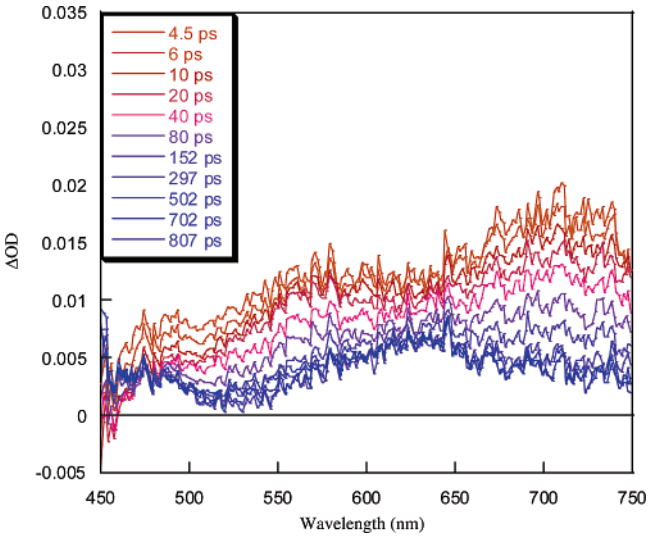

Figure 4. Transient absorption spectra of S-bonded $[Ru(tpy)(pic)(dmso)]^+$ in propylene carbonate solution at selected time delays.

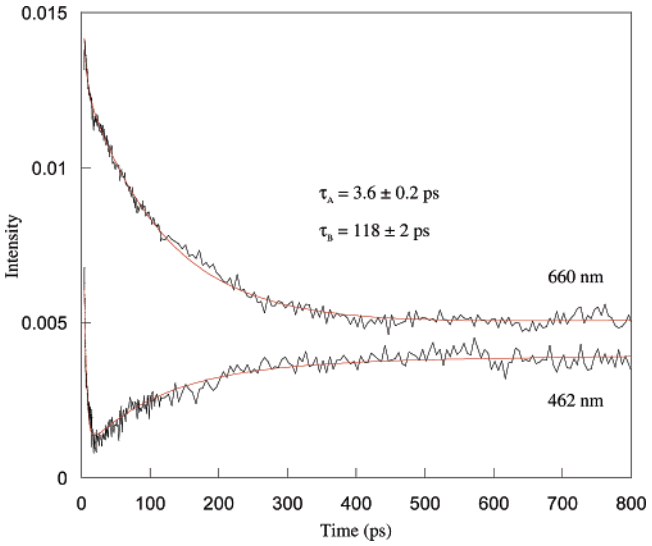

Figure 5. Single-wavelength kinetic traces (black) and biexponential fit (red) from global fitting analysis of $[Ru(tpy)(pic)(dmso)]^+$.

ps. The final trace, at 900 ns, features a bleach near 520 nm. This bleach corresponds to the O-bonded ground-state absorption (518 nm). There are no further changes in the transient absorption spectra after 900 ps. The excited-state lifetime of *O*-$[Ru(tpy)(pic)(dmso)]^+$ is 3.6 ± 0.1 ns, as measured by nanosecond transient absorption spectroscopy (Supporting Information).

Discussion

$[Ru(tpy)(bpy)(dmso)]^{2+}$. The picosecond transient absorption data of $[Ru(tpy)(bpy)(dmso)]^{2+}$ should reveal features attributable to both *S*-$[Ru(tpy)(bpy)(dmso)]^{2+*}$ and *O*-$[Ru(tpy)(bpy)(dmso)]^{2+*}$ states. The lifetime of *O*-$[Ru(tpy)(bpy)(dmso)]^{2+*}$ was independently determined to be 8.3 ± 0.1 ns. The S-bonded ground state is not observed, as it serves as the background absorption. The early time traces (up to 14 ps) show both the growing intensity of the bleach near 450 nm and the red-shifting of this feature. In addition, the sharp peak at 550 nm diminishes in intensity and shifts to lower energy. The features in the bleach region correspond to formation of the ^{3}MLCT state, whereas the absorptions in the red are attributable to $\pi^*\leftarrow\pi^*$ transitions on the reduced ligand and LMCT transitions.[32−34] The early time progression affects both of these spectral regions, and it seems reasonable to assign this 2.4 ± 0.2 ps time constant to ^{3}MLCT formation. Typically, evolution of ^{3}MLCT states is complete within 200−400 fs in $[Ru(bpy)_3]^{2+}$ and related complexes.[2−4] The lower symmetry of $[Ru(tpy)(bpy)(dmso)]^{2+}$ may contribute to the relatively slow ^{3}MLCT evolution. However, recent ultrafast dynamic studies of $[Ru(bpy)_2(Sq)]^+$ (Sq is the deprotonated form of semiquinone) show ^{3}MLCT formation to be complete in ∼300 fs.[35] Alternatively, splitting within the t_{2g} set may result in slow intersystem crossing due to decreased spin−orbit coupling.[36] Evidence for picosecond ^{3}MLCT formation was observed in $Ru^{II}-Ru^{II}$, $Os^{II}-Os^{II}$, and $Ru^{II}-Os^{II}$ bipyridine−tetrapyridophenazine dyads, in which an unassigned time constant of ∼1.6 ps was determined.[37] In these cases, red-shifts in the bipyridine-localized ^{3}MLCT bleach were observed prior to relaxation to a lower-energy phenazine-localized ^{3}MLCT.

In contrast to the charge-transfer spectral region, observation of picosecond dynamics in the red region (λ > 500 nm) of the spectrum is much more common. A similar time constant for an excited-state absorption near 530 nm with comparable band shape and position has been monitored in the ultrafast dynamics of $[Ru(dmb)_3]^{2+}$ (dmb is 4,4′-dimethyl-2,2′-bipyridine) and $[Ru(dpb)_3]^{2+}$ (dpb is 4,4′-diphenyl-2,2′-bipyridine).[3,38−40] In both examples, time constants of 2.0 ± 0.5 ps ($[Ru(dpb)_3]^{2+}$) and 5.0 ± 0.5 ps ($[Ru(dmb)_3]^{2+}$) were observed and assigned to vibrational cooling of the ligand-centered (^{3}LC) excited state.[3] Thermalization in both cases follows ^{1}MLCT → ^{3}MLCT surface crossing. It was posited that the faster relaxation for the phenyl-substituted complex relative to the methyl-substituted complex was evidence that phenyl rotations more efficiently quench the excited-state kinetic energy.[3] More recent studies of $[Ru(bpy)_3]^{2+}$ have also shown the presence of a 2−5 ps phase that has been assigned to both relaxation of higher-lying CT states and interligand electron transfer (electron localization).[5−7] It is unlikely that the spectral changes at these wavelengths in *S*-$[Ru(tpy)(bpy)(dmso)]^{2+*}$ could be due to interligand electron transfer. The distinct differences in the one-electron reduction potentials ($E^{o\prime}$, Table 1) of $bpy^{0/-}$ and $pic^{-/2-}$ and the similarity in the time constant for these complexes (pic, 3.6 ps) disfavors this assignment. One would expect that, if interligand electron transfer were involved, the time constant would not be similar for the bipyridine and picolinate Ru−dmso complexes. That the spectral changes at 460 and 550 nm in *S*-$[Ru(tpy)(bpy)(dmso)]^{2+*}$ track suggests a common spectroscopic origin. The fast 2.4 ± 0.2 ps process is assigned to evolution of *S*-^{3}MLCT and to unspecified LMCT transitions.

(32) Creutz, C.; Chou, M.; Netzel, T. L.; Okumura, M.; Sutin, N. *J. Am. Chem. Soc.* **1980**, *102*, 1309−1319.
(33) Berger, R. M.; McMillin, D. R. *Inorg. Chem.* **1988**, *27*, 4245−4249.
(34) Braterman, P. S.; Song, J.-I.; Peacock, R. D. *Inorg. Chem.* **1992**, *31*, 555−559.
(35) Ramakrishna, G.; Jose, D. A.; Kumar, D. K.; Das, A.; Palit, D. K.; Ghosh, H. N. *J. Phys. Chem. B* **2006**, *110*, 10197−10203.
(36) Siddique, Z. A.; Yamamoto, Y.; Ohno, T.; Nozaki, K. *Inorg. Chem.* **2003**, *42*, 6366−6378.
(37) Chiorboli, C.; Rodgers, M. A. J.; Scandola, F. *J. Am. Chem. Soc.* **2003**, *125*, 483−491.
(38) Damrauer, N. H.; Boussie, T. R.; Devenney, M.; McCusker, J. K. *J. Am. Chem. Soc.* **1997**, *119*, 8253−8268.
(39) Curtright, A. E.; McCusker, J. K. *J. Phys. Chem. A* **1999**, *103*, 7032−7041.
(40) Damrauer, N. H.; McCusker, J. K. *Inorg. Chem.* **1999**, *38*, 4268−4277.

The longer time (14−250 ps) transient data for *S*-[Ru(tpy)(bpy)(dmso)]$^{2+}$* show that further changes are evident. The intense bleach near 450 nm diminishes in intensity and yields to a spectrum having a shallow minimum centered near 475 nm with a long, broad featureless absorption in the red. The red portion of the spectrum is nearly identical to that observed for [Ru(tpy)$_2$]$^{2+}$* on a 50 ps time scale, produced from 532 nm excitation.[41] It is also comparable to the spectrum obtained following bulk electrolysis of [Ru(tpy)(bpy)(dmso)]$^{2+}$ at −1.3 V vs Ag/AgCl (Supporting Information). In the absence of S→O isomerization, it is expected that the negative peak near 450 nm will return to the zero line or background absorbance, indicating relaxation to the ground-state S-bonded isomer. The changing transient spectra, in conjunction with an isosbestic point, suggest direct formation of a new complex from relaxed ^{3}MLCT *S*-[Ru(tpy)(bpy)(dmso)]$^{2+}$. The most reasonable assignment for the new complex is *O*-[Ru(tpy)(bpy)(dmso)]$^{2+}$*. This assignment is affirmed upon examination of the transient absorption spectra of *O*-[Ru(tpy)(bpy)(dmso)]$^{2+}$ (Supporting Information). These spectra show a monoexponential decay on a short time scale (τ = 10 ps) to yield the O-bonded excited state. The similarity of the 250 ps time traces in both experiments is compelling. In consideration of the observed time constant (36 ps) for *S*-[Ru(tpy)(bpy)(dmso)]$^{2+}$* decay and the quantum yield for isomerization ($\Phi_{S\rightarrow O}$ = 0.024), the S→O isomerization time constant must be 1.5 ± 0.2 ns ($k_{S\rightarrow O}$ = (6.67 ± 0.04) × 10^8 s^{-1}). This analysis reveals that relaxation from *S*-[Ru(tpy)(bpy)(dmso)]$^{2+}$* to *S*-[Ru(tpy)(bpy)(dmso)]$^{2+}$ occurs in ∼35 ps at room temperature in propylene carbonate solution. Incidentally, these rates are in agreement with our original estimate determined from low-temperature single-crystal emission experiments.[23] Despite the low quantum yield of isomerization ($\Phi_{S\rightarrow O}$ = 0.024), the spectrum observed at 242 ps is attributable to excited-state *O*-[Ru(tpy)(bpy)(dmso)]$^{2+}$.

The absorption and emission data as well as the electrochemical and transient absorption data can now be compiled in an electronic state diagram for [Ru(tpy)(bpy)(dmso)]$^{2+}$ (Figure 6). The energy scale is in reference to Ag/AgCl (V), and the *x*-axis is the isomerization coordinate. The ground states are shown at the appropriate energy as determined from cyclic voltammetry. Absorption maxima are shown for both *S*- and *O*-[Ru(tpy)(bpy)(dmso)]$^{2+}$. Following formation of the initial S-bonded excited state (Ru^{II}_S*), this complex relaxes to a thermally equilibrated excited state ($^3Ru^{II}_S$*) in 2.4 ps. The complex may surface-jump to ground-state *S*-[Ru(tpy)(bpy)(dmso)]$^{2+}$ or isomerize to yield the O-bonded excited state ($^3Ru^{II}_O$*), with a time constant of 1.50 ns. For *O*-[Ru(tpy)(bpy)(dmso)]$^{2+}$, direct excitation yields thermally equilibrated $^3Ru^{II}_O$* from an initial excited state with a time constant of 10 ps. The O-bonded excited state relaxes to the ground state in 8.3 ns, as measured by nanosecond transient absorption spectroscopy. Finally, metastable *O*-[Ru(tpy)(bpy)(dmso)]$^{2+}$ relaxes to *S*-[Ru(tpy)(bpy)(dmso)]$^{2+}$ in approximately 700 s (k = 1.4 × 10^{-3} s^{-1}).

[Ru(tpy)(pic)(dmso)]$^+$. The quantum yield of S→O isomerization for [Ru(tpy)(pic)(dmso)]$^+$ is larger ($\Phi_{S\rightarrow O}$ = 0.25) than that determined for [Ru(tpy)(bpy)(dmso)]$^{2+}$ ($\Phi_{S\rightarrow O}$ = 0.024), indicating that the S→O isomerization rate constant should be greater. The lifetime of *O*-[Ru(tpy)(pic)(dmso)]$^+$* is 3.6 ns, as measured by nanosecond transient absorption spectroscopy, indicating that primarily *S*-[Ru(tpy)(pic)(dmso)]$^+$* and *O*-[Ru(tpy)(pic)(dmso)]$^+$* will be observed on the picosecond time scale. However, given the time delays for the experiment (up to 1300 ps), the O-bonded excited-state decay (3.6 ns), and the larger quantum yield for isomerization, it is clear that the formation of ground-state *O*-[Ru(tpy)(pic)(dmso)]$^+$ must be included in the analysis, as it be will be ∼30% complete within 1.3 ns.

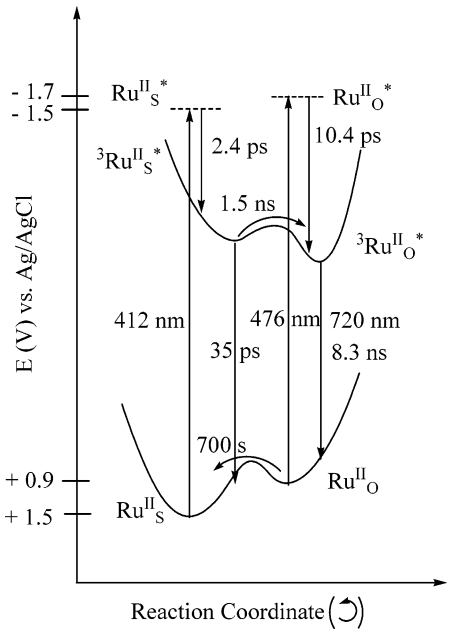

Figure 6. Electronic state diagram and rate constants for photochromic [Ru(tpy)(bpy)(dmso)]$^{2+}$.

The time constants obtained from global analysis for the spectral changes at 462 and 660 nm are 3.6 ± 0.2 and 118 ± 2 ps as well as 5.9 ns (Figure 5). Similar to the bpy complex, the fast time constant (3.6 ps) is assigned to the formation of the *S*-^{3}MLCT. The trend in the spectra is qualitatively similar to that for the bipyridine complex. The initial spectra shift to lower energy, and a bleach grows in intensity near 460 nm (5−10.0 ps). The shifts in the red region of the spectrum are more subtle but do indicate dynamics on a time scale similar to that of the bipyridine complex. Two distinct peaks are observed in the red region at 560 and 720 nm. These peaks are assigned to interligand $\pi^*\leftarrow\pi^*$ transitions on the reduced terpyridine (^{3}-LC) and LMCT transitions.[32−34] On a longer time scale ($20 < t < 800$ ps), the presence of an isosbestic point, the disappearance of the weak bleach near 460 nm, and the formation of a new transient indicate the production of a new complex. In accord with the assignment in the bpy complex, this new complex is attributed to *O*-[Ru(tpy)(pic)(dmso)]$^+$*. These spectral features are analogous to those of the bpy complex, and it is reasonable to assign the second time constant to the sum of electronic relaxation to ground-state and isomerization processes. The red region of the spectrum progresses from two distinct peaks to a single peak at 640 nm. The spectral changes on these long time scales ($t > 20$ ps) likely do not involve vibrational cooling of ^{3}LC states but represent surface crossing from the S-bonded manifold to the O-bonded manifold. The spectrum of the thermally relaxed *O*-^{3}MLCT is similar to that obtained from spectroelectrochemistry following reduction of

(41) Winkler, J. R.; Netzel, T. L.; Creutz, C.; Sutin, N. *J. Am. Chem. Soc.* **1987**, *109*, 2381−2392.

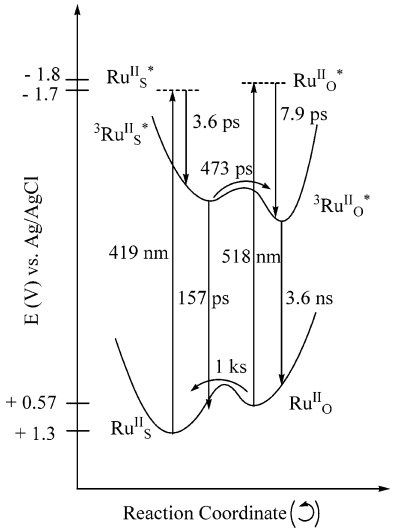

Figure 7. Electronic state diagram and rate constants for photochromic $[Ru(tpy)(pic)(dmso)]^+$.

$[Ru(tpy)(pic)(dmso)]^+$ at −1.4 V vs Ag/AgCl. This spectrum is in accord with literature spectra of $[Ru(tpy)_2]^+$ (reduced $[Ru(tpy)_2]^{2+}$) and [Li(tpy)].[33,34] In conjunction with $\Phi_{S\rightarrow O}$, an excited-state S→O isomerization time constant of 473 ± 3 ps and direct *S*-^{3}MLCT decay to ground state of 157 ± 3 ps are determined. Consistent with the increase in quantum yield, the isomerization rate constant is greater for the pic complex ($k = (2.11 \pm 0.2) \times 10^9\ s^{-1}$) than for the bpy complex ($k = (6.65 \pm 0.2) \times 10^8\ s^{-1}$). From the spectra of photoconverted *O*-$[Ru(tpy)(pic)(dmso)]^+$, the evolution of *O*-^{3}MLCT is biexponential, with $\tau = 8.0 \pm 0.2$ ps and 4.0 ± 0.2 ns. It is unclear why ^{3}MLCT formation for both O-bonded excited states is so slow, but it may involve movement of the O-bonded dmso ligand. Relaxation of *O*-^{3}MLCT to metastable *O*-$[Ru(tpy)(pic)(dmso)]^+$ occurs with a time constant of 3.6 ns. The slowest time constant (5.9 ns) obtained from the triexponential model of the picosecond transient absorption spectra is assigned to decay of *O*-$[Ru(tpy)(pic)(dmso)]^{+}$* to *O*-$[Ru(tpy)(pic)(dmso)]^+$ and matches well with what is observed on the nanosecond time scale (3.6 ns).

In Figure 7 is shown an energy diagram which summarizes all of the results for $[Ru(tpy)(pic)(dmso)]^+$. The absorption maxima and $Ru^{3+/2+}$ couples are determined from electronic spectroscopy and electrochemical studies, respectively. Following excitation of *S*-$[Ru(tpy)(pic)(dmso)]^+$ to form an initial excited state, relaxation to a thermally equilibrated excited state (S-^{3}MLCT) occurs in 3.6 ps. Both isomerization to *O*-$[Ru(tpy)(pic)(dmso)]^{+}$* ($\tau = 473$ ps) and deactivation to *S*-$[Ru(tpy)(pic)(dmso)]^+$ ($\tau = 157$ ps) occur from this state. The lifetime of *O*-$[Ru(tpy)(pic)(dmso)]^{+}$* is 3.6 ns, yielding metastable *O*-$[Ru(tpy)(pic)(dmso)]^+$. This metastable state ultimately produces ground-state *S*-$[Ru(tpy)(pic)(dmso)]^+$ in 1000 s ($k = 1 \times 10^{-3}\ s^{-1}$).

The differences in the rates of isomerization are due to an increased coupling of O-^{3}MLCT with S-^{3}MLCT in $[Ru(tpy)(pic)(dmso)]^{+}$* relative to $[Ru(tpy)(bpy)(dmso)]^{2+}$*. Previously, we noted that isomerization involves dmso rotation about the Ru−S bond and suggested a dynamic role for the picolinate ligand in which the carboxylate oxygen helps push the dmso away from ruthenium(III) in the excited state.[28] Isomerization is further promoted by a repulsive steric interaction with the methyl groups of dmso and the 6-H of bipyridine or picolinate experienced during rotation of dmso about the Ru−S bond. It is curious to consider that the isomerization barrier must be smaller for the pic complex, despite the stronger Ru−S bond for the pic complex relative to the bpy complex (bpy, d(Ru−S) = 2.282 Å; pic, d(Ru−S) = 2.215 Å). It is also interesting to note that, despite the presumed weaker ligand field for the pic complex, excited-state decay on the S-bonded surface is more rapid for the bpy complex. As the kinetic analysis above notes, the time constant for decay on the S-bonded surface is shorter for the bpy complex (37 ps) than for the pic (157 ps) complex. This is confusing, since the standard model for decay in ruthenium polypyridine complexes suggests more rapid decay time constants for complexes containing weaker ligand fields.[1] A weaker ligand field is more strongly coupled with the ^{3}MLCT states, resulting in more rapid excited-state deactivation due to an increased nonradiative decay constant (k_{nr}). In accord with this model, the lifetime of $[Ru(bpy)_2(pic)]^+$ is 120 ns in deoxygenated acetonitrile, dramatically reduced from ∼1.0 μs in the same medium for $[Ru(bpy)_3]^{2+}$.[42] Our experimentally determined lifetime of 150 ns for this complex is consistent with this literature report. However, the disparate lifetimes of $[Ru(tpy)(bpy)(dms)]^{2+}$ ($\tau = 250$ ps; dms is dimethyl sulfide) and *trans*-$[Ru(tpy)(pic)(dms)]^+$ ($\tau = 6.5$ ns) indicate that the reversal of trend is not relegated just to the dmso complexes (Supporting Information). This latter example is notable in that the sulfide complexes should adhere to the standard model, especially since isomerization is not a potential reaction pathway. Thus, it appears not only that the isomerization rate constant is increased for the pic complex but also that the excited-state decay rate constant is decreased. Both of these factors, in conjunction with the dynamical effects mentioned earlier, lead to a greater isomerization quantum yield. That the analogous dmso and dms complexes show similar excited-state behavior suggests a more fundamental change in the electronic structure of the pic complex relative to the bpy complex.

A common strategy to extend ^{3}MLCT lifetimes in transition metal complexes is to engineer a triplet ligand-centered excited state (^{3}LC) energetically close to an emissive ^{3}MLCT.[43−45] In the presence of coupling between these two states, energy transfer leads to a lengthened ^{3}MLCT lifetime. In the absence of two emissive states within a complex, detection of such an effect is best achieved via transient absorption spectroscopy. It is compelling to invoke just such an interaction between a ^{3}LC state from picolinate and the ^{3}MLCT from *S*-$[Ru(tpy)(pic)(dmso)]^{+}$*, leading to a lengthened excited-state lifetime for both *S*-$[Ru(tpy)(pic)(dmso)]^{+}$* and $[Ru(tpy)(pic)(dms)]^{+}$*. The O-bonded surfaces are energetically isolated from ^{3}LC picolinate states, preventing observation of this effect for those complexes. Recall that the lifetimes of *O*-$[Ru(tpy)(bpy)(dmso)]^{2+}$* and *O*-$[Ru(tpy)(pic)(dmso)]^{+}$* are similar. Alternatively, the origin of the long excited-state lifetimes in pic complexes with dms and dmso may involve an unspecified synergistic bonding

(42) Norrby, T.; Borje, A.; Akermark, B.; Hammarstrom, L.; Alsins, J.; Lashgari, K.; Norrestam, R.; Martensson, J.; Stenhagen, G. *Inorg. Chem.* **1997**, *36*, 5850−5858.
(43) Baitalik, S.; Wang, X.-Y.; Schmehl, R. H. *J. Am. Chem. Soc.* **2004**, *126*, 16304−16305.
(44) Wang, X.-Y.; Guerzo, A. D.; Schmehl, R. H. *J. Photochem. Photobiol. C* **2004**, *5*, 55−77.
(45) Cattaneo, M.; Fagalde, F.; Katz, N. E.; Leiva, A. M.; Schmehl, R. *Inorg. Chem.* **2006**, *45*, 127−136.

interaction associated with the π-donor carboxylate moiety trans to the π-stabilizing dms or dmso. This interaction would impart greater ligand character in the ground state, resulting in a destabilization of the e_g* orbital set greater than anticipated. This effect would be inoperative in the bpy complexes since the ligand trans to dmso is a π-stabilizing pyridine moiety. Computational studies may be able to detect this effect.

A second interesting feature of the transient spectra of [Ru(tpy)(bpy)(dms)]$^{2+}$ and *trans*-[Ru(tpy)(pic)(dms)]$^{+}$ is that the fast 2−4 ps ^{3}MLCT evolution is not observed, occurring on a faster time scale. This conspicuous absence prompts the notion that this kinetic phase in the dmso complexes may involve orientation of dmso to obtain a critical isomerization geometry, a point alluded to earlier. It is expected that the thermally relaxed excited-state structure not only exhibits a weaker Ru−S bond than that observed in the Franck−Condon state but also features twists and rotations of the dimethyl sulfoxide ligand. This observation further supports our LMCT assignment of the early dynamics in the red region of the spectrum. Motions involving the bound dmso ligand are expected to alter transitions having metal character, while having little influence on ^{3}LC transitions having no metal character. The effect of this molecular motion reasonably leads to lengthened time constants for formation of ^{3}MLCT states.

Conclusions

We have presented data that support nanosecond and picosecond S→O isomerization of bound dmso in [Ru(tpy)(bpy)(dmso)]$^{2+}$ and *trans*-[Ru(tpy)(pic)(dmso)]$^{+}$. These fast isomerization rates and large isomerization quantum yields are indicative of electronic structures which efficiently access the stored potential energy within a ^{3}MLCT excited state. This energy is required for the molecular rearrangement associated with isomerization. Future results will focus on isomerization of chelating sulfoxides as well as additional picosecond transient absorption measurements to improve our understanding of these transformations.

Acknowledgment. We thank Michael Jensen, Hugh Richardson of Ohio University, and Russell Schmehl of Tulane University for helpful discussions as well as Dr. E. O. Danilov for experimental assistance and the Ohio Laboratory for Kinetic Spectrometry for access to the picosecond transient absorption spectrometer utilized in these studies. PRF (38071-G3), Ohio University (1804 Fund), and the Condensed Matter Surface Science Program are acknowledged for financial support.

Supporting Information Available: Kinetic plots and picosecond transient absorption spectra of *O*-[Ru(tpy)(pic)(dmso)]$^{+}$ and *O*-[Ru(tpy)(bpy)(dmso)]$^{2+}$ as well as nanosecond (pic) and picosecond (bpy) transient absorption spectra of [Ru(tpy)(pic)(dms)]$^{+}$ and [Ru(tpy)(bpy)(dms)]$^{2+}$. This material is available free of charge via the Internet at http://pubs.acs.org.

JA0641305